12th International Conference on Fracture Mechanics of Concrete and Concrete Structures
FraMCoS-12
B.L.A. Pichler, Ch. Hellmich, P. Preinstorfer (Eds)

https://doi.org/10.21012/FC12.1306
MS07-2:5

EFFECTS OF BRINE AND CO_2 EXPOSURE ON THE MECHANICAL AND CHEMICAL PROPERTIES OF CLASS G CEMENT IN OIL WELL APPLICATIONS

ANDERSON V. NEVES*, VICTOR N. LIMA† AND FLÁVIO A. SILVA‡

* Department of Civil and Environmental Engineering, Pontifícia Universidade Católica do Rio de Janeiro
Rua Marquês de São Vicente 225, 22451-900, Rio de Janeiro, Brazil
e-mail: avneves@puc-rio.br, www.puc-rio.br

† Department of Energy and Petroleum Engineering, University of Stavanger
P. O. Box 8600, 4036 Stavanger, Norway
e-mail: victor.nogueiralima@uis.no, www.uis.no

‡ Department of Civil and Environmental Engineering, Pontifícia Universidade Católica do Rio de Janeiro
Rua Marquês de São Vicente 225, 22451-900, Rio de Janeiro, Brazil
e-mail: fsilva@puc-rio.br, www.puc-rio.br

Key words: Class G cement, Oil well cementing, Brine and CO_2 exposure, Mechanical properties, Triaxial testing

Abstract. Cementing is one of the most critical stages in oil well construction, as it ensures the proper fixation of the casing and prevents fluid migration through permeable zones. Class G cement, used in this process, is subjected to harsh conditions, particularly at great depths, where both temperatures and pressures are elevated. Exposure to brine and CO_2 under extreme conditions can compromise the durability of the cement and the well's integrity by altering its physical, chemical, and mechanical properties. Given the significance of these factors, it is essential to investigate their influence on the cement sheath. This study exposed Class G cement samples for three months in autoclaves under high pressure (20 MPa) and temperature (88 °C) in environments saturated with brine and brine with CO_2. Uniaxial and triaxial compression tests, porosity analysis, X-ray diffraction, and pH measurements were conducted. The results showed that confining pressure significantly impacted samples exposed to brine+CO_2, leading to plastic deformations at pressures above 20 MPa, even before the application of deviatoric stresses. Exposure to brine+CO_2 reduced compressive strength by 45% compared to the reference samples, likely due to micro defects forming during curing and chemical reactions with acidic gases. To determine whether the contribution of micro defect formation caused by the loading and unloading during the curing procedure was more significant than the chemical reactions, samples cured under the same pressure and temperature conditions but exposed only to brine were tested. The results showed that the reduction in strength and alterations in the material's elastic properties were more closely related to the adopted curing procedure than to the chemical reactions resulting from the acidic environment.

1 INTRODUCTION

Primary cementing in oil well construction is a fundamental operation following the drilling phase. After positioning the steel casing in the wellbore, a cement slurry is injected into the annular space between casings or between the

casing and surrounding rock formation. This slurry solidifies over time, forming a cement sheath that plays a crucial role in ensuring well integrity. The cement sheath serves multiple essential functions, including zonal isolation, casing corrosion protection, and providing mechanical support [1]. The primary goal of this barrier material is to withstand in-situ stresses, temperature gradients, and chemical exposure, maintaining structural integrity to effectively seal off potential leakage pathways [2]. Failure to maintain cement sheath integrity may lead to issues such as annular pressure buildup, gas migration to shallow formations or the surface, and, in severe cases, blowouts with significant infrastructure damage [3].

Researchers have extensively studied cement slurry performance under in-situ conditions to identify factors influencing barrier efficacy. In cases where the cement encounters acidic gases like H_2S and CO_2, durability concerns emerge. Such exposure may induce mechanical weakening, alter hydration products, and increase porosity and permeability [4, 5]. Given the increasing emphasis on CCUS (Carbon Capture, Utilization, and Storage) research, investigating how cement responds to degradation by acidic gases has gained notable importance [4, 6–8].

Most research on chemical interactions among CO_2, brine, and well barrier materials has centered on Portland cement due to their common use in well construction and abandonment operations and their high reactivity in CO_2-rich environments [9–11]. Previous studies have shown rapid reactions between calcium-containing cement phases, notably portlandite, and CO_2-saturated brine, with the diffusion of reactants and products constraining hydration alterations [12]. This leads to distinct reaction fronts in the cement, resulting in various zones, including unaltered cement, a portlandite-depleted zone, a calcium carbonate zone, and a residual amorphous silica zone [13, 14].

When CO_2 is introduced, it reduces the pH and dissolves phases such as portlandite (CH), calcium silicate hydrate (C-S-H), and other minor phases, significantly affecting the cement's chemical stability [13, 15]. The dissolution of portlandite, typically faster than that of C-S-H, results in a portlandite-depleted zone that precipitates calcium carbonate, filling smaller pores and decreasing overall porosity, potentially clogging the pore space [16]. Conversely, carbonation processes may reduce pore connectivity, although cases of pore network expansion are observed due to silica gel formation from C-S-H decomposition [17].

Mechanical stresses within a well are also pivotal in determining leakage risks, as they influence dynamic flow within fractures [1]. In acid gas leakage, interactions among cement, steel, rock, and CO_2-laden brine may alter fracture properties, leading to fracture closure and reduced permeability due to chemical changes [14]. Thus, a holistic evaluation integrating mechanical and chemical behavior is essential for understanding well integrity under coupled geochemical and geomechanical conditions.

This study systematically investigates class G cement cured under high-pressure and high-temperature conditions, focusing on its response to CO_2 exposure. The experimental program is structured into three phases: an initial characterization (including porosimetry and brine pH analysis), a mechanical assessment (with uniaxial and triaxial compression tests), and a chemical evaluation (using X-ray diffraction).

2 EXPERIMENTAL PROGRAM

2.1 Materials and mixing

In this study, a cement paste mix was formulated using Class G oil well cement to achieve a target compressive strength of 50 MPa after 28 days. This mix was stabilized with specific additives for fluid loss control and to mitigate the surfactant effects of the primary fluid loss additive. Details on the additive types were previously discussed in studies by [18, 19] and the mixing proportion is summarized in Table 1. The Class G cement used has a Blaine fineness of 2738 cm^2/g and a density of 3.19 g/cm^3.

Table 1: Class G cement paste mix composition. In the table, bwoc represents the proportion of additives based on the weight of cement, and w/c represents the ratio of water to cement in the mix.

Materials	Manufacturer	Proportion
Class G cement	Lafarge Holcim	-
Deionized water	-	0.44 w/c
Fluid loss	Kuraray	0.4% bwoc
Deforamer	BASF	0.1% bwoc

The mixing process adhered to API 10A [20] and API 10B [21] standards, with a water-to-cement ratio of 0.44, and involved quality checks on parameters such as free water content, thickening time, and early compressive strength, as outlined in [8]. Mixing was performed using a Chandler model 3260 mixer with the following protocol: (a) adding water and liquid additives to the vessel, (b) pre-blending cement and powdered additives, (c) incrementally adding the dry mixture at 4000 RPM for 15 seconds, and (d) mixing at 12,000 RPM for an additional 35 seconds.

Test specimens were prepared in cylindrical molds with dimensions of 50 mm diameter × 100 mm height for mechanical tests, and 25.4 mm diameter × 50 mm height for porosimetry measurements. Specimens were cured in water for 14 days to minimize shrinkage-induced cracking and ensure optimal mechanical test results, given that the mix typically achieved over 80% of its strength by this time, as per [18]. On the fourteenth day, specimens for brine and brine+CO_2 exposure underwent porosimetry analysis.

For the long-term aging assessment, specimens brine-exposed and brine+ CO_2-exposed were conditioned in a curing chamber under a pressure of 20 MPa and a temperature of 88 °C for three months. This procedure aimed to simulate the conditions of an oil well at a depth of 3000 m, following protocols adapted from [22–24]. The saline solution was prepared according to ASTM D1141-98 to replicate seawater and introduced into the autoclave at an approximate brine-to-sample volume ratio of 0.8, considering the autoclave's total capacity of 10 liters. For the specimens brine-exposed, the autoclave was sealed after being filled with the brine solution, and the target temperature and pressure conditions were applied. In contrast, for specimens subjected to brine+ CO_2 exposure, the brine was first saturated with 100% gaseous CO_2 after sealing the autoclave. The initial sample molding was conducted at the Pontifical Catholic University of Rio de Janeiro, while the degradation tests in the autoclave were carried out at the National Institute of Technology (INT – Rio de Janeiro), as detailed in [8].

After long-term aging, 25.4 × 50 mm samples were analyzed via gas expansion porosimetry at PUC-Rio to assess degradation impacts. Chemical analyses of the brine solution were also conducted. The experimental protocol involved characterizing reference, brine-exposed, and brine-CO_2-exposed cement pastes using porosimetry, X-ray diffraction, unconfined compressive strength tests, and confined compression tests at varying confining pressures.

2.2 Porosity measurements

The porosity analysis involved helium expansion techniques to determine grain and pore volumes within the samples. Measurements were conducted with a Corelab Ultrapore 300 helium expansion porosimeter, using three samples per cement paste type: reference, brine-exposed, and brine+CO_2-exposed. Each sample had a 25.4 mm diameter and 50 mm height, tailored for this study. To reduce moisture interference, samples were dried in a desiccator at a vacuum pressure of 760 torr for 24 hours. This approach aligns with prior methodology validation [8, 18].

2.3 Brine pH measurements

A brine solution was formulated at the National Institute of Technology (INT – Brazil)

following the composition specified in Table 2. This solution was then stored in a PVC cylindrical container. Once transferred to the autoclave, the pH of the solution was measured using a Digimed model DM-22 pH meter, which had been calibrated and certified by INMETRO, Brazil's regulatory authority.

Table 2: Brine solution composition.

Compound	Value g	Concentration g/L
$MgCl_2.6H_2O$	3889.0	555.6
$CaCl_2$(anhydrous)	405.6	57.9
$SrCl_2.6H_2O$	14.8	2.1

2.4 Mechanical tests

The mechanical testing, including uniaxial and triaxial behavior, was carried out using the MTS model 815 machine, which offers a compression load capacity of 2700 kN and can apply a confining pressure of up to 80 MPa. The system was equipped with an MTS Flex Test 60 controller, along with two axial strain gauges and one circumferential strain gauge, ensuring precise control of the test procedure and accurate data acquisition. Prior to the tests, the specimens were carefully prepared by applying self-fusing silicone electrical tape and a heat-shrinkable FEP membrane, which prevented direct contact between the confining fluid and the specimen, thereby reducing the risk of damage that could influence the material's mechanical properties. In addition, two axial and one circumferential extensometer were attached to the specimen, as shown in Figure 1.

For the unconfined compression strength tests, the circumferential displacement of the sample was maintained at a strain rate of 5×10^{-5} min^{-1} until failure was observed. As described by Lima et al. [25], this approach enabled the study of post-peak behavior, with failure occurring in a controlled manner. During the confined tests, the specimen was positioned similarly to the uniaxial tests and placed into a triaxial vessel, which was then sealed and filled with Mobil Mobiltherm 605 fluid. Once the triaxial cell was fully filled, confining pressure was gradually applied at a rate of 2.5 MPa/min until it reached target values of 10, 20, or 40 MPa. Each of these conditions was tested on three separate samples. The tests were conducted under undrained conditions, where the pore fluid was retained within the specimen, potentially influencing its mechanical strength. However, as noted in prior research [18], this effect was previously explored and addressed.

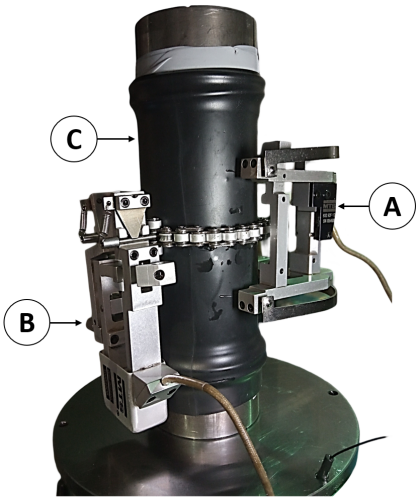

Figure 1: Compression strength test setup illustrating key components: axial extensometer (A), circumferential extensometer (B), and black heat-shrinkable membrane (C). The membrane is applied to protect the cement sample from oil contamination, ensuring reliable results in triaxial tests.

2.5 X-ray diffraction

Analytical evaluations were performed on powdered samples from both reference and exposed specimens. The sample preparation involved breaking the specimens into smaller pieces with a hammer, followed by grinding with a mortar and pestle, and finally sieving through a 500-mesh sieve. After preparation, the powdered samples were reserved for X-ray diffraction (XRD) analysis.

XRD patterns of class G cement pastes were recorded using a Bruker D8 Discover diffractometer, with Cu Kα radiation set to 40 kV and

40 mA. This setup included a Ni filter and Lynx-Eye detector, operating in Bragg-Brentano geometry across a 2θ range of 10° to 90°, with a step size of 0.02°. Data collection times were optimized to ensure a minimum of 5,000 counts at the most intense peak. Quantitative mineralogical analysis was achieved through Rietveld refinement using fundamental parameters, performed with TOPAS 5.0 software (Bruker AXS, Germany). Additional details and statistical parameter from the Rietveld refinement method can be found in [8].

3 RESULTS AND DISCUSSIONS

3.1 Porosity results

The values obtained through porosity measurements of the reference, and brine+CO_2-exposed, and brine-exposed samples are, respectively, 7.11 ± 0.27%, 25.53 ± 5.04%, and 19.82 ± 4.25%. The results indicated that a substantial increase in porosity values was observed in the post-exposed samples, regardless of the presence of acid gas. According to previous studies [26, 27], one possible explanation for this increase in porosity of the samples exposed to the combination of brine and CO_2 may be related to bicarbonate reactions and leaching processes, which enhance porosity and permeability. In the case of samples exposed only to brine, the explanation may be associated with the portlandite dissolution and leaching of calcium from the C–S–H structure [28]. Both of these processes lead to a loss of mechanical strength, and this behavior will be discussed afterward [27, 28].

3.2 Mechanical tests results

Compression strength tests were performed under undrained conditions for all samples analyzed, adhering to rock mechanics conventions where compressive stresses and strains are considered positive. While this discussion emphasizes confined cases, it is essential to first highlight the uniaxial compressive strength (UCS) values obtained for the three tested groups: 55.55 ± 2.06 MPa for the reference samples, 27.03 ± 1.87 MPa for brine+CO_2-exposed samples, and 25.64 ± 2.45 MPa for brine-exposed samples. These UCS results provide a critical baseline for evaluating the impact of exposure conditions and play a pivotal role in the subsequent analysis of the magnitude of the applied confining pressure. Understanding these initial conditions is key to interpreting the material's behavior under varying confinement scenarios and offers insight into the damage mechanisms affecting strength performance.

Figure 2a illustrates the stress-strain behavior for both axial ($\varepsilon_{ax} = \varepsilon_z$) and lateral ($\varepsilon_{lat} = \varepsilon_x = \varepsilon_y$) deformations of the reference and exposed cement paste samples. The results demonstrated high reproducibility among the three sample groups, with a low coefficient of variation observed for compressive strength and estimated elastic properties, including Young's modulus and Poisson's ratio. For clarity, only the intermediate curve from the three tested samples is displayed for each case.

The data reveal that even a modest confining pressure of 10 MPa significantly enhanced the ductility of the cement paste samples, allowing deformations to extend beyond the failure range observed in the unconfined sample results (less than 0.75% axial strain). The reference cement paste displayed moderate frictional reinforcement as confining pressure increased. In contrast, samples exposed to acidic gas (CO_2) exhibited pronounced plastic deformation at 10 MPa and demonstrated strain hardening behavior at higher confining pressures of 20 and 40 MPa, as highlighted previously by [8]. For samples exposed exclusively to brine, the failure behavior was similar to that of the reference samples, though their compressive strength was markedly lower.

These observations highlight the influence of the initial curing process, during which the samples were subjected to pressure and atmospheric temperature conditions before autoclave treatment, leading to both chemical and mechanical alterations [29]. As noted by Meng et al. [30], traditional curing methods have inherent drawbacks; the cooling and depressurization cycles, followed by reheating and repressurization, can

introduce micro-defects and residual stresses that compromise the mechanical properties of the cement. Consequently, the observed reduction in strength for both exposed groups is likely linked to damage induced by these pressure and temperature cycles. These findings emphasize the critical role of curing protocols in preserving the structural integrity of cementitious materials under extreme conditions.

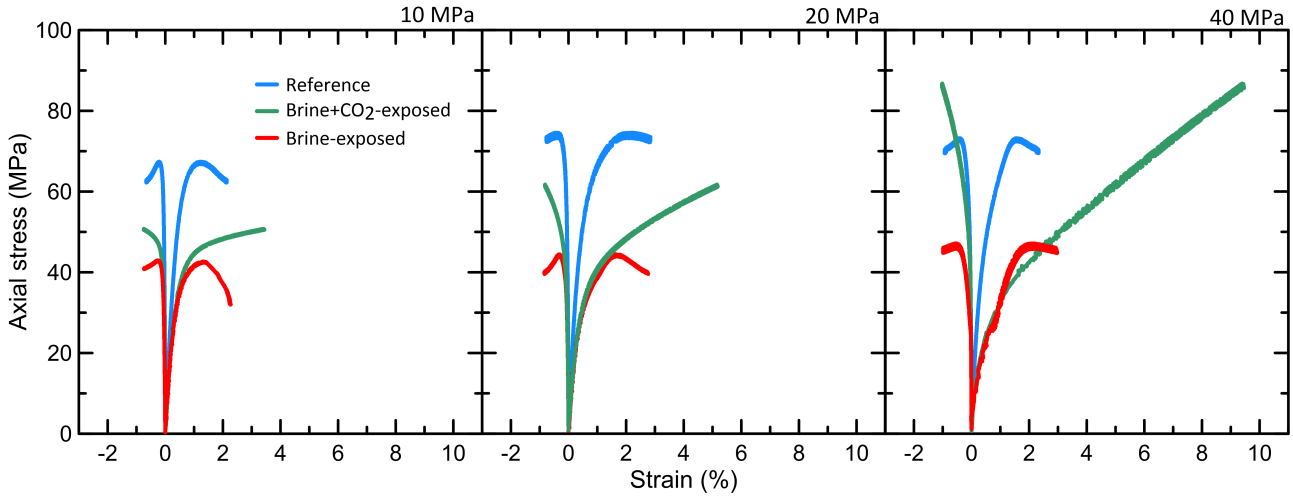

(a)

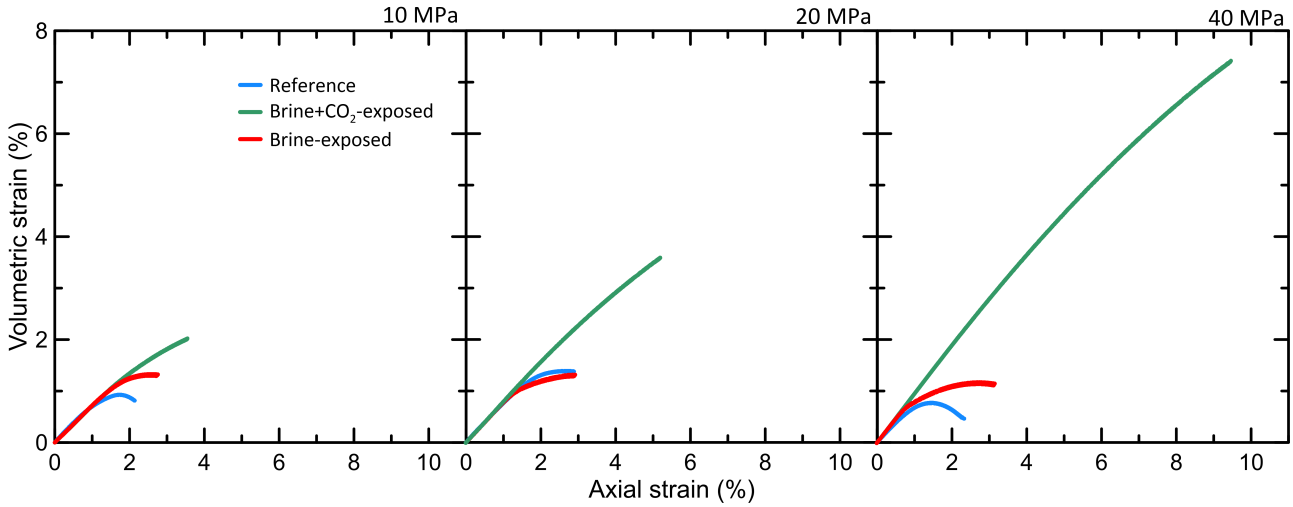

(b)

Figure 2: Confined compression strength test results. (a) Axial stress x strain behavior; (b) Volumetric strain x axial strain behavior.

Table 3: Summary of elastic properties for specimens tested under confined conditions.

Sample	Confining pressure (MPa)	E (GPa)	ν	$Pc/\sigma_{max,UCS}$
Reference	10	15.7	0.10	0.18
	20	14.9	0.09	0.36
	40	14.7	0.11	0.72
Brine+CO_2	10	10.5	0.14	0.37
	20	8.7	0.1	0.74
	40	6.7	0.04	1.48
Brine	10	10.3	0.13	0.39
	20	8.2	0.09	0.78
	40	6.8	0.06	1.56

Table 3 summarizes the measured elastic properties, including Young's modulus (E), Poisson's ratio (ν), and the ratio of confining pressure to uniaxial compressive strength ($Pc/\sigma_{max,UCS}$). Prior studies on comparable oil well cement pastes under similar confinement conditions have shown that elastic moduli tend to decrease with increasing confining pressure [18, 31]. Consistent with these findings, our results indicate that the elastic moduli for all three sample groups are influenced by confining pressure, with a modest reduction of approximately 5% observed. However, a more pronounced effect was observed for the samples exposed to brine+CO_2 and brine. Under a confining pressure of 40 MPa, these samples exhibited significant reductions in Young's modulus, reaching approx. 40%. This substantial decrease can be attributed to the $Pc/\sigma_{max,UCS}$ ratio, which, at higher values, generates hydrostatic pressures that exceed the material's deviatoric strength, potentially leading to bulk structural damage. This phenomenon is further corroborated by the observed rapid transition from the elastic to plastic behavior, as shown in Figure 2a, where $Pc/\sigma_{max,UCS} > 1$ plays a critical role.

Figure 3 presents the correlation between confining pressure and volumetric strain for all groups subjected to triaxial testing. For the exposed samples (Brine and Brine+CO_2), a notable transition from a linear to a nonlinear response occurs at confining pressures exceeding 20 MPa. This shift indicates that the material experiences damage during the confinement phase, as further supported by the $Pc/\sigma_{max,UCS}$ ratio. The observed damage is reflected in the deviatoric stress versus axial strain behavior depicted in Figure 2. These findings suggest that the transition point marks a critical phase in the material's mechanical response, where the interplay between confining pressure and internal microstructural changes significantly influences deformation characteristics.

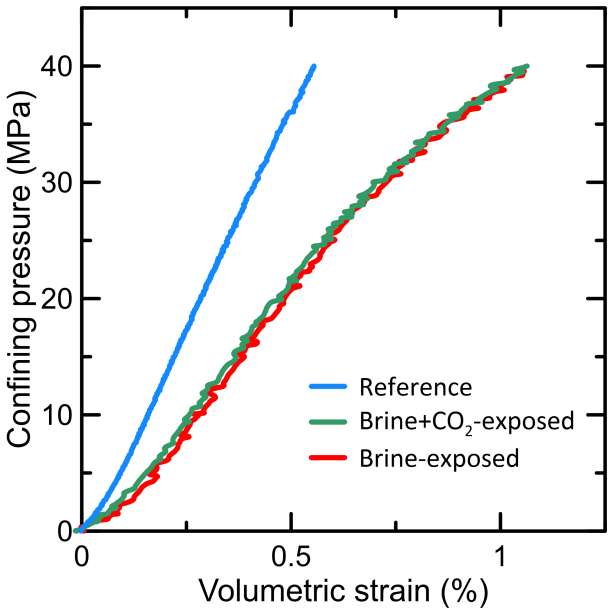

Figure 3: Relationship between confining pressure and volumetric strain.

3.3 X-ray diffraction and brine pH results

The diffraction patterns of the reference Class G cement paste and the test specimens exposed to brine+CO_2, replicating conditions found in a 3000-meter-deep oil well, are illustrated in Figure 4. The phases identified, along with their mass proportions derived from Rietveld refinement analysis, are summarized in Table 4.

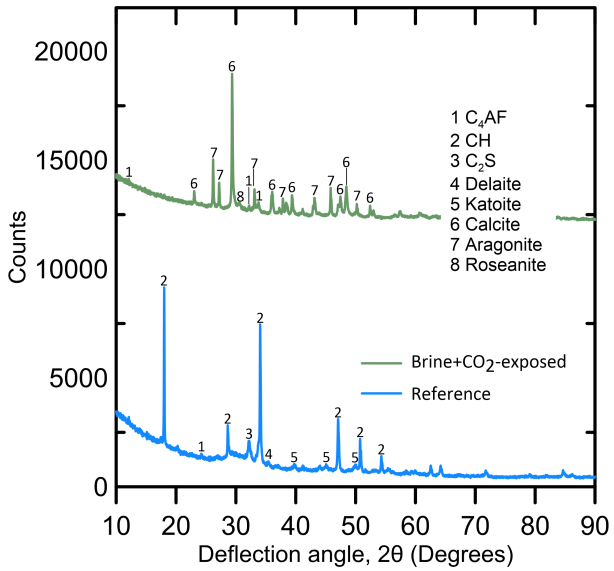

Figure 4: X-ray diffraction analysis highlighting the cement phase peaks, comparing the reference case with the brine + CO_2 exposure scenario.

Table 4: Summary of the crystalline phases and mass proportions obtained by the Rietveld refinement analysis.

Phase	Reference	Brine+CO_2
C_2S	22.4	-
C_4AF	16.1	10.3
C-S-H	39.8	27.6
Portlandite	15.1	-
Calcite	6.6	37.4
Aragonite	-	24.7
Adjustment parameters		
Rwp	4.01	5.16
GOF	1.42	1.39

For samples exposed to CO_2, the diffraction patterns revealed calcite ($CaCO_3$) as the primary crystalline phase formed during exposure. This aligns with findings by Omosebi et al. [27], who reported that carbonation of C–S–H results in the formation of calcite, aragonite, and vaterite—three polymorphs of $CaCO_3$. The appearance of aragonite and vaterite is associated with significant decalcification of C–S–H, which is intensified by elevated calcium ion concentrations [29]. Increased exposure to CO_2 accelerates the carbonation process, with excess $CaCO_3$ forming due to the dissolution of calcium hydroxide (CH). As Castellote et al. [32] noted, this process explains the minimal portlandite (CH) content observed in the diffraction analyses of exposed samples.

The kinetics of carbonation are governed by exposure conditions and microstructural characteristics. Carbonation of hydrated cement paste induces notable changes in porosity and pore size distribution, consistent with prior reports [26, 27, 32]. Porosity measurements indicated a significant increase in CO_2-exposed samples, which aligns with the literature. This increase can be attributed to CO_2 dissolution in water as HCO_3^- or CO_3^{2-}, leading to a reduction in brine pH [33]. The lower pH enhances the dissolution of Ca^{2+} ions into the brine, which then diffuse out of the pores and precipitate on the sample's surface as $CaCO_3$ due to the elevated Ca^{2+} concentration [29]. This calcium leaching weakens the cement's mechanical properties [26, 27].

Cement paste exposed to CO_2-saturated brine undergoes a complex interplay of processes, including hydration, chemical shrinkage, thermally induced expansion, pressure-induced structural transformations of calcium silicates, decalcification, carbonation, and mineral leaching. These processes collectively alter porosity, mechanical strength, chemical composition, and brine pH, consistent with observations by other researchers [27, 34]. However, it is noteworthy that the reaction zone caused by exposure to acidic gases is limited to the sample's external layers, which alone cannot fully account for the observed loss in mechan-

ical properties. This points once again to the curing method as a contributing factor.

In addition to X-ray diffraction analysis, the pH of the brine solution was measured to further characterize its interaction with the cement samples and correlate it with the crystalline phase analysis. Initially, the solution's pH was recorded at 8.25 at 25°C. After exposure of the first sample group to brine+CO_2 gas, the pH dropped to 7.18 at 25°C, and the solution appeared transparent. This reduction in alkalinity is consistent with prior findings [15, 27, 29, 34] and supports the enhanced dissolution of Ca^{2+} ions in the brine solution, as discussed above and highlighted by other authors.

4 CONCLUSION

These findings underscore the susceptibility of cementitious materials to mechanical degradation under high confining pressures, especially when combined with exposure to chemically aggressive environments. The interplay between confining pressure and elastic moduli highlights the importance of considering both mechanical and chemical factors when evaluating the performance of cementitious materials in demanding subsurface conditions, such as those encountered in oil well applications.

Based on the previous statement, the following conclusions stem from the analyses presented in this study:

- The porosity measurements revealed a significant increase in post-exposure samples, irrespective of the presence of CO_2, with values rising from 7.11% in the reference samples to 25.53% and 19.82% in the brine+CO_2-exposed and brine-exposed samples, respectively. This increase is attributed to mechanisms such as carbonation and calcium leaching, highlighting the impact of chemical interactions on porosity and mechanical strength.

- Compression strength tests revealed a significant reduction in uniaxial compressive strength (UCS) for brine-exposed (25.64 ± 2.45 MPa) and brine+CO_2-exposed (27.03 ± 1.87 MPa) samples compared to reference samples (55.55 ± 2.06 MPa). This strength reduction is attributed to chemical alterations, including carbonation reactions, leaching of calcium from portlandite and the C–S–H matrix, and increased porosity induced by exposure to aggressive environments. These processes compromise the microstructure, reducing load-bearing capacity. Under confined conditions, a modest pressure of 10 MPa significantly enhanced ductility for all groups, with CO_2-exposed samples demonstrating pronounced plastic deformation and strain hardening at higher pressures (20 and 40 MPa).

- X-ray diffraction and Rietveld refinement analysis revealed significant changes in the crystalline phases of cement paste exposed to CO_2-saturated brine, including the complete depletion of portlandite and the formation of calcite (37.4%) and aragonite (24.7%). These changes are attributed to carbonation and decalcification processes, driven by the dissolution of calcium hydroxide (CH) and calcium silicate hydrates (C–S–H). The reduction in brine pH from 8.25 to 7.18 further highlights the aggressive chemical environment, accelerating calcium ion leaching and carbonate precipitation.

5 ACKNOWLEDGEMENTS

This study was financed in part by the Coordenação de Aperfeiçoamento de Pessoal de Nível Superior – Brazil (CAPES) – Finance Code 001 and by the Brazilian funding agencies FAPERJ and CNPq. The authors would like to acknowledge Lafarge-Holcim for the donation of class G cement, BASF for the donation of the defoamer and Kuraray for the donation of the Kuraray Poval™ additive. This research is a collaboration work between PUC-Rio, Norwegian Research Centre AS and the University of Stavanger. The experimental work has been

partially carried out with the use of the Laboratory LAH2S at the National Institute of Technology (INT-Brazil).

V. N. Lima acknowledges The Research Council of Norway for financing the Centre for Research-based Innovation SWIPA – Centre for Subsurface Well Integrity, Plugging and Abandonment, RCN project number 309646. The centre is also financed by the operating companies AkerBP, Equinor ASA and Harbour Energy, and includes in addition more than 20 in-kind contributing industry partners. The R&D partners in SWIPA are SINTEF, NORCE, IFE, NTNU and the University of Stavanger.

REFERENCES

[1] E. B. Nelson and D. Guillot, *Well cementing*, vol. 2. Sugar Land, Texas, USA: Newnes, 2006.

[2] T. Vrålstad, J. Todorovic, A. Saasen, and R. Godøy, "Long-term integrity of well cements at downhole conditions," in *SPE Norway Subsurface Conference?*, p. D011S004R003, SPE, 2016.

[3] N. Agofack, S. Ghabezloo, J. Sulem, A. Garnier, and C. Urbanczyk, "Experimental investigation of the early-age mechanical behaviour of oil-well cement paste," *Cement and Concrete Research*, vol. 117, pp. 91–102, 2019.

[4] O. Omosebi, R. Ahmed, S. Shah, and S. Osisanya, "Mechanical Integrity of Well Cement Under Geologic Carbon Sequestration Conditions," *CMTC Carbon Management Technology Conference*, vol. All Days, pp. CMTC–439562–MS, 11 2015.

[5] J. F. Zhang, J. L. Yang, K. Liu, B. Wang, and R. X. Hou, "Carbon dioxide corrosion and corrosion prevention of oil well cement paste matrix in deep wells," *Applied Mechanics and Materials*, vol. 692, pp. 433–438, 2014.

[6] N. Agbasimalo and M. Radonjic, "Experimental Study of Portland Cement/Rock Interface In Relation to Wellbore Stability For Carbon Capture And Storage (CCS)," *U.S. Rock Mechanics/Geomechanics Symposium*, vol. All Days, pp. ARMA–2012–206, 06 2012.

[7] M. Tiong, R. Gholami, and Y. Li, "A Novel Portland Cement for CO2 Sequestration by Nanoparticles," *IPTC International Petroleum Technology Conference*, vol. Day 3 Wed, February 23, 2022, p. D032S152R003, 02 2022.

[8] A. V. Neves, V. N. Lima, I. N. Lima, S. Letichevsky, R. R. de Avillez, and F. de Andrade Silva, "The influence of h2s and co2 on the triaxial behavior of class g cement paste under elevated temperature and pressure," *Geoenergy Science and Engineering*, p. 213084, 6 2024.

[9] J. W. Carey, M. Wigand, S. J. Chipera, G. WoldeGabriel, R. Pawar, P. C. Lichtner, S. C. Wehner, M. A. Raines, and G. D. Guthrie, "Analysis and performance of oil well cement with 30 years of co2 exposure from the sacroc unit, west texas, usa," *International Journal of Greenhouse Gas Control*, vol. 1, no. 1, pp. 75–85, 2007. 8th International Conference on Greenhouse Gas Control Technologies.

[10] N. J. Huerta, B. R. Strazisar, S. L. Bryant, and M. A. Hesse, "Time-dependent fluid migration from a storage formation via leaky wells," *Energy Procedia*, vol. 63, pp. 5724–5736, 2014. 12th International Conference on Greenhouse Gas Control Technologies, GHGT-12.

[11] H. E. Mason, W. L. D. Frane, S. D. C. Walsh, Z. Dai, S. Charnvanichborikarn, and S. A. Carroll, "Chemical and mechanical properties of wellbore cement altered by co2-rich brine using a multianalytical approach," *Environmental Science*

& Technology, vol. 47, pp. 1745–1752, 2 2013. doi: 10.1021/es3039906.

[12] B. G. Kutchko, B. R. Strazisar, S. B. Hawthorne, C. L. Lopano, D. J. Miller, J. A. Hakala, and G. D. Guthrie, "H2s–co2 reaction with hydrated class h well cement: Acid-gas injection and co2 co-sequestration," *International Journal of Greenhouse Gas Control*, vol. 5, no. 4, pp. 880–888, 2011.

[13] S. Carroll, J. W. Carey, D. Dzombak, N. J. Huerta, L. Li, T. Richard, W. Um, S. D. Walsh, and L. Zhang, "Review: Role of chemistry, mechanics, and transport on well integrity in co2 storage environments," *International Journal of Greenhouse Gas Control*, vol. 49, pp. 149–160, 2016.

[14] S. D. Walsh, H. E. Mason, W. L. Du Frane, and S. A. Carroll, "Experimental calibration of a numerical model describing the alteration of cement/caprock interfaces by carbonated brine," *International Journal of Greenhouse Gas Control*, vol. 22, pp. 176–188, 2014.

[15] V. Papadakis, M. Fardis, and C. Vayenas, "Effect of composition, environmental factors and cement-lime mortar coating on concrete carbonation," *Materials and Structures*, vol. 25, no. 5, p. 293 – 304, 1992. Cited by: 152.

[16] M. Arandigoyen, B. Bicer-Simsir, J. Alvarez, and D. Lange, "Variation of microstructure with carbonation in lime and blended pastes," *Applied Surface Science*, vol. 252, no. 20, pp. 7562–7571, 2006.

[17] V. Ngala and C. Page, "Effects of carbonation on pore structure and diffusional properties of hydrated cement pastes," *Cement and Concrete Research*, vol. 27, no. 7, pp. 995–1007, 1997.

[18] V. N. Lima, H. J. Skadsem, K. Beltrán-Jiménez, A. Zhemchuzhnikov, R. Q. Velloso, and F. de Andrade Silva, "Triaxial behavior of a stabilized and a highly porous oil well cement paste at different saturation and drainage conditions," *Journal of Petroleum Science and Engineering*, vol. 219, p. 111055, 2022.

[19] V. N. Lima, H. J. Skadsem, F. R. Souza, T. Kaneshima, S. Letichevsky, R. R. de Avillez, and F. A. Silva, "Effects of Noncrosslinked Polyvinyl Alcohol Fluid Loss Additive on the Compressive Strength and Viscosity of Class G Cement Slurries," *SPE Journal*, vol. 29, pp. 3516–3530, 07 2024.

[20] API, "API 10A: Specification for Cements and Materials for Well Cementing," 2011.

[21] API, "10B-2: Recommended Practice for Testing Well Cements.," 2013.

[22] G. Lende, J. A. Clausen, and A. J. Kvassnes, "Evaluation of new innovative cement blend for enhanced co2 and h2s resistance," in *SPE/IADC Drilling Conference and Exhibition*, p. D031S009R003, SPE, 2021.

[23] J. Todorovic, N. V. Opedal, B. Werner, J. Angelique Clausen, and A. Jæger Sweetman Kvassnes, "Effect of Long-Term Aging in Carbonated Brine on Mechanical Properties of a Novel Cement System with an Expandable Agent," *SPE Norway Subsurface Conference*, vol. Day 1 Mon, November 02, 2020, p. D011S004R004, 11 2020.

[24] A. Garnier, J. B. Laudet, S. Patil, R. Patil, K. Ravi, and L. Ferreira, "Effect of Acid Gas on Cement Sheath Integrity: Experimental Findings," *SPE Kingdom of Saudi Arabia Annual Technical Symposium and Exhibition*, vol. All Days, pp. SPE–160890–MS, 04 2012.

[25] V. N. Lima, F. d. A. Silva, H. J. Skadsem, K. Beltrán-Jiménez, and J. K. Sunde, "Effects of confinement pressure on the mechanical behavior of an oil well cement paste," *Journal of Petroleum Science and Engineering*, vol. 208, p. 109769, jan 2022.

[26] R. A. Bruckdorfer, "Carbon dioxide corrosion in oilwell cements," *SPE Rocky Mountain Regional Meeting*, pp. SPE–15176–MS, 05 1986.

[27] O. Omosebi, R. Ahmed, and S. Shah, "Mechanisms of cement degradation in hpht carbonic acid environment," in *SPE International Conference on Oilfield Chemistry*, OnePetro, 2017.

[28] F.-J. Ulm, E. Lemarchand, and F. H. Heukamp, "Elements of chemomechanics of calcium leaching of cement-based materials at different scales," *Engineering Fracture Mechanics*, vol. 70, no. 7, pp. 871–889, 2003.

[29] B. Šavija and M. Luković, "Carbonation of cement paste: Understanding, challenges, and opportunities," *Construction and Building Materials*, vol. 117, pp. 285–301, 2016.

[30] M. Meng, L. Frash, J. W. Carey, W. Li, and N. Welch, "Measurement of cement in-situ mechanical properties with consideration of poroelasticity," *SPE Journal*, vol. 27, pp. 2655–2667, 10 2022.

[31] R. Lorenzoni, V. N. Lima, T. C. S. Figueiredo, M. Hering, S. Paciornik, M. Curbach, V. Mechtcherine, and F. de Andrade Silva, "Macro and meso analysis of cement-based materials subjected to triaxial and uniaxial loading using x-ray microtomography and digital volume correlation," *Construction and Building Materials*, vol. 323, p. 126558, 2022.

[32] M. Castellote, L. Fernandez, C. Andrade, and C. Alonso, "Chemical changes and phase analysis of opc pastes carbonated at different co2 concentrations," *Materials and Structures/Materiaux et Constructions*, vol. 42, pp. 515–525, 5 2009.

[33] M. J. Mitchell, O. E. Jensen, K. A. Cliffe, and M. M. Maroto-Valer, "A model of carbon dioxide dissolution and mineral carbonation kinetics," *Proceedings of the Royal Society A: Mathematical, Physical and Engineering Sciences*, vol. 466, pp. 1265–1290, 5 2010.

[34] Y. Li, T. Mi, W. Liu, Z. Dong, B. Dong, L. Tang, and F. Xing, "Chemical and mineralogical characteristics of carbonated and uncarbonated cement pastes subjected to high temperatures," *Composites Part B: Engineering*, vol. 216, p. 108861, 2021.